POLITECNICO DI TORINO
Repository ISTITUZIONALE

Body Dust: Ultra-Low Power OOK Modulation Circuit for Wireless Data Transmission in Drinkable sub-100m-sized Biochips

Original
Body Dust: Ultra-Low Power OOK Modulation Circuit for Wireless Data Transmission in Drinkable sub-100m-sized Biochips / Luca Barbruni, G., MOTTO ROS, P., Aiassa, S., Demarchi, D., Carrara, S.. - (2019).

Availability:
This version is available at: 11583/2782313 since: 2020-01-19T19:11:14Z

Publisher:
arXiv

Published
DOI:

Terms of use:

This article is made available under terms and conditions as specified in the corresponding bibliographic description in the repository

Publisher copyright

(Article begins on next page)

18 November 2026

arXiv:1912.02670v1 [physics.ins-det] 5 Dec 2019

Body Dust: Ultra-Low Power OOK Modulation Circuit for Wireless Data Transmission in Drinkable sub-100µm-sized Biochips

Gian Luca Barbruni*†, Paolo Motto Ros‡, Simone Aiassa*†, Danilo Demarchi*†, Sandro Carrara†
*Department of Electronics and Telecommunications, Politecnico di Torino, Turin, Italy
†Integrated Circuits Laboratory, École Polytechnique Fédérale de Lausanne, Neuchâtel, Switzerland
‡Electronic Design Laboratory, Istituto Italiano di Tecnologia, Genova, Italy
Corresponding author: simone.aiassa@polito.it

***Abstract*—In this paper, we discuss the feasibility of creating an UltraSound (US) communication circuit to wireless transmit outside the body diagnostic information from multiplexed biosensors chip built on the top layer of a drinkable CMOS Body Dust cube. The system requires to be small enough (lateral size of less than 100 µm) to mimic the typical size of a larger blood cell (diameter around 30 µm for white cells) and so support free circulation of the cube in human tissues. The second constraint came from the low-power consumption requirement, with the energy provided by an external US base station. The results of the feasibility study demonstrate the possibility to design an architecture for a data transmission transponder by using a 0.18 µm CMOS process, with sub-10 µW of power consumption and a total chip area of 43x44 µm^2. The paper also discusses the limits of the designed system and the need for further improvements toward real applications in Body Dust diagnostics.**

I. Introduction

The Body Dust proposed approach [1] has the target to develop highly innovative solutions for precision medicine applications, to obtain a more efficient and preventive diagnosis, for example in oncology. The system to be implemented is an ingestible micro-active sensing-chip with a wireless connection to an external base station, namely, through an UltraSound (US) communication system. The in-body biochip is conceived to answer by reflecting back a portion of the interrogating US wave by backscattering modulation. A similar approach has been followed by [2] in which a US LSK modulator for deep implanted medical devices has been realized. In our work, the transducer model comes from [2], [3], because of its equal f0 operating frequency and its scalability in dimensions, required in the presented application. In the Body Dust system, the battery-less transponder retrieves a DC power supply by rectifying the incoming US signal. The literature suggests that through this method the power transfer achieves only a few µW for the operation of the entire chip [4], being power consumption a crucial point to determine tag performance. Considering the target application, the Body Dust chip must present a lateral size of less than 100 µm. Recent results in literature indicate that is possible to realize CMOS microsystems at these sizes. In particular, a complete CMOS IC for multi-purpose sensing was realized in 2014 [5] with a total size of 0.36 mm^2, while a 2.5 µm radius working electrode was realized for biosensing [6], and a micro-coils with 50 µm of later size was published in 2016 [7]. This work presents a CMOS architecture to transmit the maximum number of information outside the body through On-Off Keying (OOK) modulation for backscattering. Similar transmissions have been proposed in 2013 for Neural Dust sensing approach [8], where the system included three nodes, an external transceiver, a subdural one, and the proper Neural Dust device. Meanwhile, in our design, only two components are expected, which are the body dust tag and the external base station which works both as power transmitter and as data receiver. Moreover, [8] is lacking a communication circuit and the impedance modulation is achieved through switching MOSFET only. Although in this work, we include a communication protocol to transmit outside the information. We base our design on an end-to-end, from the sensor read-out front-end to the transmitter back-end, event-driven digital architecture. The event-based approach aims in at pursuing an improved quality-energy trade-off [9] and has been already showed promising results in this specific application [10].

II. Proposed Architecture

The presented work here focuses on the design of the CMOS circuit for communication, highlighting both the resulting size and power consumption. The proposed system contains a 1 MHz Starved Ring Oscillator (SRO), a front-end monostable, a monostable synchronizer, a 4-in Parallel-Input

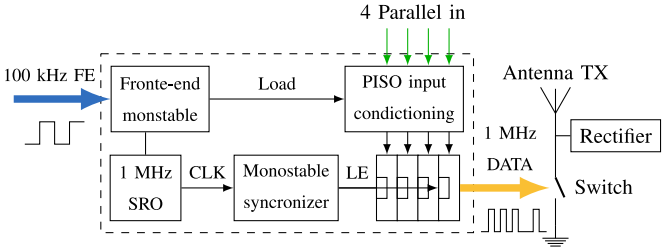


Fig. 1: System block diagram.

Serial-Output (PISO) register, and a modulator switch (Fig. 1). The biosensor front-end is described in [1]. A potentiostat on the top metal layer followed by an I-to-f (Current to frequency) converter, translate the biochemical information in a quasi-digital format. The quasi-digital signal is a digital signal carrying an analog information, already implemented for low power biosensing [11], and it could directly trigger an event-driven wireless transmitter (e.g. an impulse radio [12]). This signal is considered here as the input of the proposed circuit. Since here we have to distinguish among different sensor front-end types, each event is labelled with a unique source identifier. This binary address is provided from the multiplexed layer of the chip that is designed to allow for at least 5 different quasi-digital signals (3 bits for the identification) to be transmitted. In [1], the I-to-F is designed with a sensitivity of 7 kHz/nA, the sensitivity of the electrochemical sensor mounted on the top metal layer almost 180 nA/(mmol·mm), and the estimated current range at the Counter Electrode is between 1 nA and 5 nA. From this, the maximum frequency of the quasi-digital signal coming from the potentiostat is considered to be 100 kHz.

A. The Starved Ring Oscillator (SRO)

The SRO generates the clock to synchronize the system and to modulate the serial output at a frequency of 1 MHz. The oscillation frequency of the SRO is approximated by (1)

$$f = \frac{I}{N \cdot C_{tot} \cdot V_{dd}} \tag{1}$$

where N is the number of stages of the ring, C_{tot} is the total capacitance, V_{dd} the power supply (1.8 V) and I the current. The here implemented topology is a three-stages-starved-ring configuration with three equal capacitors, as shown in Fig. 2.

The values of C and MOSFETs are optimized to guarantee a 1 MHz oscillation, minimizing the capacitance to reduce the final size of the chip. The selected value for C is 200 fF. By increasing the length of the transistors is possible to reduce the capacitance accordingly, but as a matter of fact, the total area improvement is less than 10 %. Further, this would negatively affect the SRO performance reliability by making the oscillation frequency highly dependent on the parasitic capacitance. After simulating different trade-off in this regard, we deemed the proposed design a safe and good solution. The SRO is tested through a post-layout simulation, sweeping the temperature from 27 °C to 47 °C, which is the typical range of biomedical application. Considering this range of temperature, the simulation results prove that the maximum shifting in frequency is 10 %. The performance of the designed oscillator are compared with similar works [13], [14] in Table I.

TABLE I: SRO performance comparison.

	[13]	[14]	This work
CMOS technology	130 nm	130 nm	180 nm
Voltage supply (V)	3.3	3.3	1.8
External component	Yes	No	No
Frequency (MHz)	22.5-360	1	1
Power (μW)	1515*	87	9.5
Area (mm^2)	0.05	0.054	0.00116

*At 200 MHz

B. The Parallel-Input Serial-Output (PISO) register

The here implemented 4-input PISO register is composed of four D-latches, triggered by a Latch Enable (LE) that is generated by the monostable synchronizer, as represented in Fig. 3. Latches are preferred than Positive Edge Triggered (PET)-D Flip Flop in order to both improve the synchronism and reduce the size. The inputs of the latches (parallel word) came from a simple combinational circuit in which the LOAD signal is triggered by the front-end monostable to control writing and shifting time. In particular, when LOAD is at the logic state high the word is written to each latch, when it is at the logic state low the PISO acts like a shift register. After four clock cycles, the serial data is ready to modulate the final MOSFET. Here the size of the transistors is the minimum provided from the selected Process Design Kit (PDK). By reducing the technology node it is possible to scale all the circuit minimizing the area. The transmitted data packet is encapsulated similarly to the work done for a wireless multi-channel event-driven tactile sensing glove [15]. As shown in Fig. 4, the packet is composed by a header (bit 1 always) to declare the starting of the transmission and three bits for the

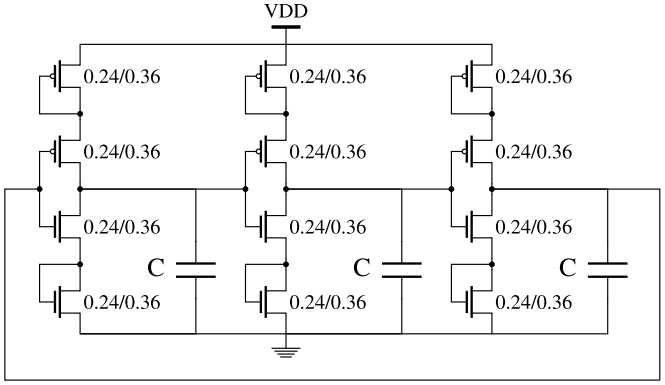


Fig. 2: Three stages starved Ring Oscillator (RO).

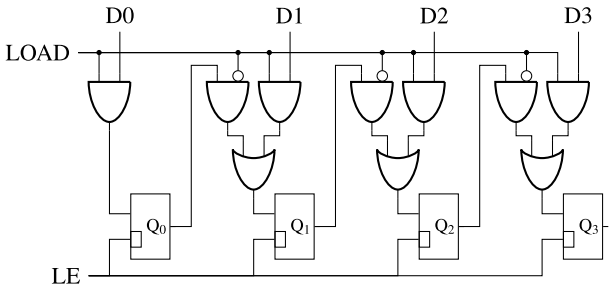


Fig. 3: Four inputs PISO register.

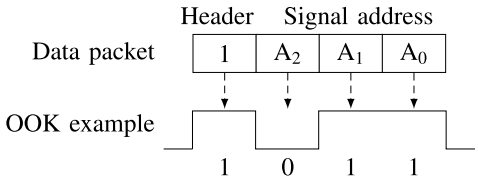


Fig. 4: Packet template and example of OOK modulation.

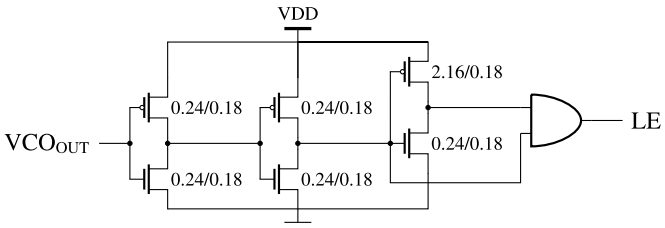


Fig. 5: Implemented monostable synchronizer.

signal address (A_2, A_1, A_0). The minimum to distinguish the 5 signals treated by the sensor front end multiplexer.

C. The Front-end Monostable

The front-end monostable receives the Front-End (FE) signal and it is composed by a D-latch as delay block. Whenever a rising edge of the incoming signal is detected, a pulse is generated as the LOAD signal that triggers the PISO Input Conditioning in the writing or shifting operations. The LOAD signal retains its logic state high enough for almost 1 µs to detect the possible variations of the parallel word coming from the multiplexed layer and to ensure that at least one edge of the clock is asserted.

D. The Monostable Synchronizer

The monostable synchronizer generates the LE signal. It is a delay block made by a chain of inverters as presented in Fig. 5. The monostable synchronizer is the most critical part of the circuit since it has to be sized accordingly to the number of components receiving the trigger, namely, four latches in the PISO register and one latch in the front-end monostable. The output LE signal is a 1 ns pulse over the activation threshold. To improve the synchronization, the monostable synchronizer is centred with respect to all the latch in the layout [16].

III. On-Off Keying (OOK) Modulator

The final On-Off Keying (OOK) modulator is implemented by a MOSFET (NMOS in particular) acting as a switch. The drain driving current is high enough to modulate the impedance of the piezoelectric transmitting antenna. The size of the transistors is chosen accordingly to the transducer electrical equivalent impedance. In the designed circuit modulator resistance (R_m) is set exactly equal in value to the resistance of the electrical model of the piezoelectric antenna [2]: when the switch is open, R_m is equal R_p, and the full matched condition is achieved. On the contrary, when the switch is closed, R_m is equal to R_{on} and the mismatched condition is achieved. The circuit is shown in Fig. 6, R_m and R_p are 3552 Ω, C_p is 62.75 pF and the current I is 10 µA.

IV. Simulation Results

To show the versatility of the proposed architecture, Fig. 7 presents the simulation of our circuit into a more complex system including the management of multiple sensors. Using two different templates (1101 and 1001) is possible to emulate the detection of two different molecules concentrations (for example glucose and lactate). To simulate the activation of two biosensors on the analog front-end and the treatment of the signals provided by the multiplexing layer, the communication circuit continuously receives the quasi-digital signal from the same FE input without any information about the type of signal. The discriminant is the signal address (A_2, A_1, A_0), provided through a counter by the multiplexer. In particular,

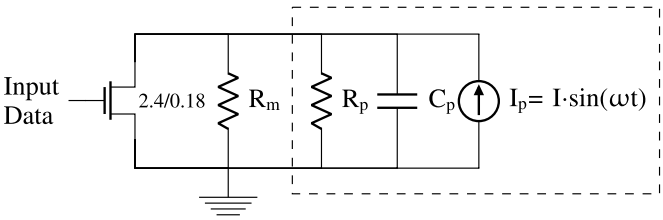


Fig. 6: Electrical model of the piezo and incident wave (red box), R_M modulator and NMOS switch.

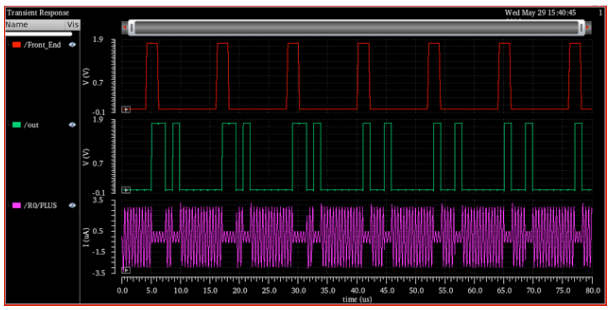
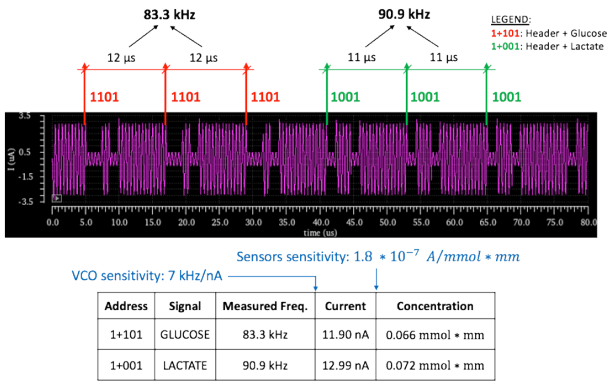


Fig. 7: Full-circuit transient analysis with two different packet templates (1101 and 1001).



Address	Signal	Measured Freq.	Current	Concentration
1+101	GLUCOSE	83.3 kHz	11.90 nA	0.066 mmol ∗ mm
1+001	LACTATE	90.9 kHz	12.99 nA	0.072 mmol ∗ mm

Fig. 8: Different frequency for two different signals extracted and modulated.

the pink wave is received at the base station (assuming the absence of the tissues as losing medium) and the information is reconstructed as highlighted in Fig. 8. This proves the functioning of the circuit and, moreover, its scalability compared to more complex multi-sensor systems. In Fig. 9 the final layout of the proposed architecture is depicted: switch and modulator are not present since they require to be tuned accordingly to other transducer models. The area breakdown of the designed architecture is shown in Fig. 10. Most of the area is occupied by the ring oscillator and the same is valid considering the power consumption. More than 95 % of the averaged power is consumed by the SRO. Nevertheless, post-layout simulation of the circuit results in the total power consumption of 9.7 µW. The instantaneous current required for the oscillation results to be 350 µA/pulse (630 µW/pulse), while 450 µA/pulse (810 µW/pulse) are spent for the total transmission. Table II presents a comparison with [2], which demonstrates that the here proposed OOK modulation based implementation shows a 80 % reduction in the average power consumption, and a 75 % lower instant power consumption.

V. Conclusion

In this paper, a novel architecture for data transmission in Body Dust diagnostics has been presented. The results of such feasibility study demonstrate the possibility to design an architecture for a US data transponder by using a 0.18 µm CMOS process, with an average power consumption of less than 10 µW and a total chip area of 43x44 µm^2. Even if we have implemented the design of a starved architecture intending to reduce both area and power consumption, the study shows that the source of major area consumption is still the ring-oscillator. Although, this is the first work to prove the feasibility of creating an architecture to wireless transmit data outside from the Body Dust cube. Additional work is still needed to further reduce the chip area, e.g. by considering smaller CMOS nodes. Even if our simulations already show promising results w.r.t ultrasound integrated communication devices, a smaller CMOS node together with subthreshold design approaches would help to further reduce the power consumption.

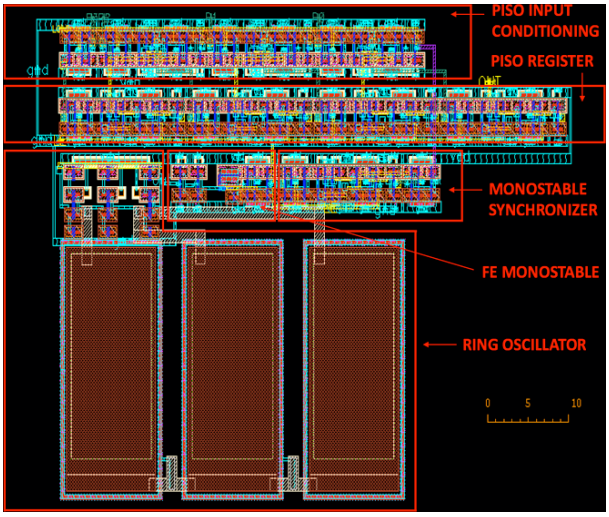


Fig. 9: Implemented circuit layout with partition of the area for each block.

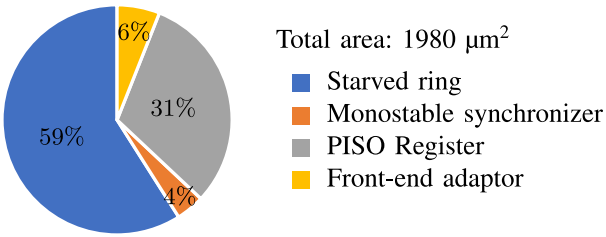


Fig. 10: Total area per block in the implemented circuit.

TABLE II: Modulation comparison.

	[2]	This work
Modulaton	FSK	ASK
Average Power (µW)	49	9.7
Instant Power (mW/pulse)	3.2	0.81

Acknowledgment

The authors would like to thank Catherine Dehollain from EPFL, Lausanne, for useful discussions about power transmission with UltraSound.

References

[1] J. Snoeijs, P. Georgiou, and S. Carrara, "CMOS body dust - Towards drinkable diagnostics," *2017 IEEE Biomedical Circuits and Systems Conference (BioCAS)*, Turin, 2017, pp. 1-4.

[2] F. Mazzilli, E. G. Kilinc, and C. Dehollain, "3.2 mW ultrasonic LSK modulator for uplink communication in deep implanted medical devices," *2014 IEEE Biomedical Circuits and Systems Conference (BioCAS)*, Lausanne, 2014, pp. 636-639.

[3] M. J. Weber, Y. Yoshihara, A. Sawaby, J. Charthad, T. C. Chang, and A. Arbabian, "A miniaturized single-transducer implantable pressure sensor with time-multiplexed ultrasonic data and power links," *IEEE Journal of Solid-State Circuits*, vol. 53, no. 4, pp. 1089-1101, 2018.

[4] F. Song, J. Yin, H. L. Liao, and R. Huang, "Ultra-low-power clock generation circuit for EPC standard UHF RDID transponders," *Electronics Letters*, vol. 44, no. 3, pp. 199-201, 2008.

[5] S. S. Ghoreishizadeh, C. Baj-Rossi, A. Cavallini, S. Carrara, and G. De Micheli, "An integrated control and readout circuit for implantable multi-target electrochemical biosensing," *IEEE Transactions on Biomedical Circuits and Systems*, vol. 8, no. 6, pp. 891-898, 2014.

[6] J. Rothe , O. Frey, A. Stettler, Y. Chen, and A. Hierlemann, Fully integrated CMOS microsystem for electrochemical measurements on 3232 working electrodes at 90 frames per second," *Analytical Chemistry*, vol. 86, no. 13, pp. 6425-6432, 2014.

[7] S. W. Lee, F. Fallegger, B. D. Casse, and S. I. Fried, "Implantable microcoils for intracortical magnetic stimulation," *Science advances*, vol. 2, no. 12, pp. e1600889, 2016.

[8] D. Seo, J. M. Carmena, J. M. Rabaey, E. Alon, and M. M. Maharbiz, "Neural dust: An ultrasonic, low power solution for chronic brain-machine interfaces," arXiv:1307.2196 [q-bio.NC], 2013.

[9] P. Motto Ros, A. Sanginario, M. Crepaldi, and D. Demarchi, "Quality-energy trade-off and bio-inspired electronic systems," *2018 IEEE International Conference on the Science of Electrical Engineering in Israel (ICSEE)*, Eilat, 2018, pp. 1-5.

[10] P. Motto Ros, B. Miccoli, A. Sanginario, and D. Demarchi, "Low-power architecture for integrated CMOS bio-sensing," *2017 IEEE Biomedical Circuits and Systems Conference (BioCAS)*, Turin, 2017, pp. 1-4.

[11] S. Aiassa, F. Stradolini, A. Tuoheti, S. Carrara and D. Demarchi, "Quasi-digital biosensor-interface for a portable pen to monitor anaesthetics delivery," *15th Conference on Ph.D Research in Microelectronics and Electronics (PRIME)*, Lausanne, 2019, pp. 265-268.

[12] M. Crepaldi, M. Stoppa, P. Motto Ros, and D. Demarchi, "An analog-mode impulse radio system for ultra-low power short-range audio streaming," *IEEE Transactions on Circuits and Systems I: Regular Papers*, vol. 62, no. 12, pp. 2886-2897, 2015.

[13] X. Yi, X. Chen, and R. Yao, "Frequency-adjustable clock oscillator based on frequency-to-voltage converter," *Electronics Letters*, vol. 45, no. 11, pp. 530-532, 2009.

[14] Z. P. Bian, and R. H. Yao, "Process, voltage and temperature compensation in a 1-MHz 130nm CMOS monolithic clock oscillator with 2.3% accuracy," *International Journal of Electronics*, vol. 102, no. 10, pp. 1652-1663, 2015.

[15] P. Motto Ros, M. Crepaldi, A. Bonanno, and D. Demarchi, "Wireless multi-channel quasi-digital tactile Sensing glove-based system," *2013 Euromicro Conference on Digital System Design*, Los Alamitos, CA, 2013, pp. 673-680.

[16] J. M. Rabaey, A. Chandrakasan, and B. Nikolic, *Digital Integrated Circuits*, 2nd ed. Englewood Cliffs: Prentice Hall, 2002.